Characterization of Very Low Intensity Ion Beams from CERN REX/HIE-ISOLDE Linear Accelerator

Niels Bidault[1,2]

[1]BE-OP-ISO, CERN, 1211 Geneva 23, Switzerland
[2]University of Rome 'La Sapienza' & INFN, 00185 Rome, Italy

February 17th, 2021.

Contents

REX-ISOLDE

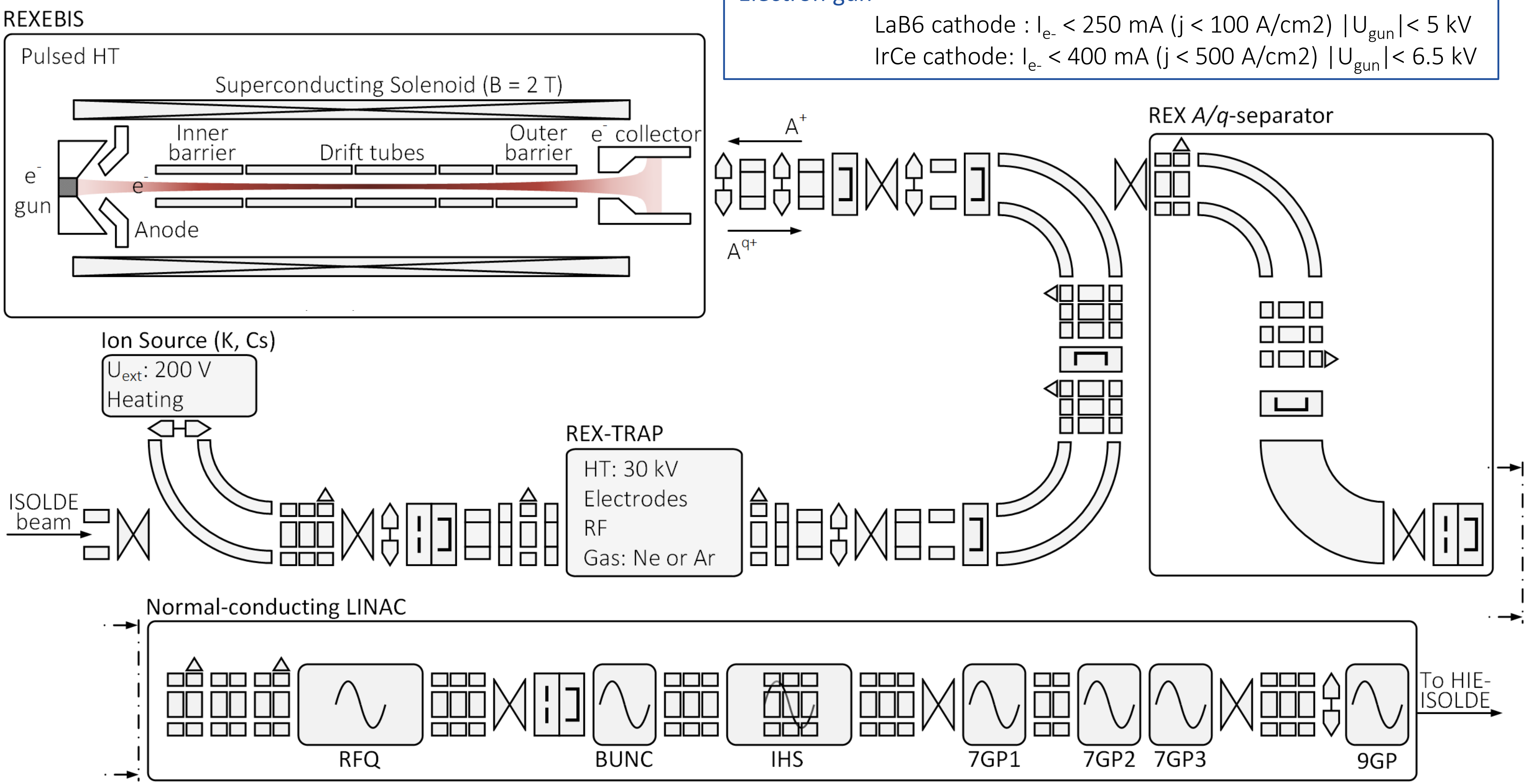

Electron gun

LaB6 cathode : I_{e-} < 250 mA (j < 100 A/cm2) $|U_{gun}|$< 5 kV

IrCe cathode: I_{e-} < 400 mA (j < 500 A/cm2) $|U_{gun}|$< 6.5 kV

HIE-ISOLDE

REX LINAC basic parameters

f = 101.28 MHz
Four-rod λ/2 RFQ and Buncher
IH-structure
Three 7-Gap resonators
9-Gap resonator (f = 202.56 MHz)

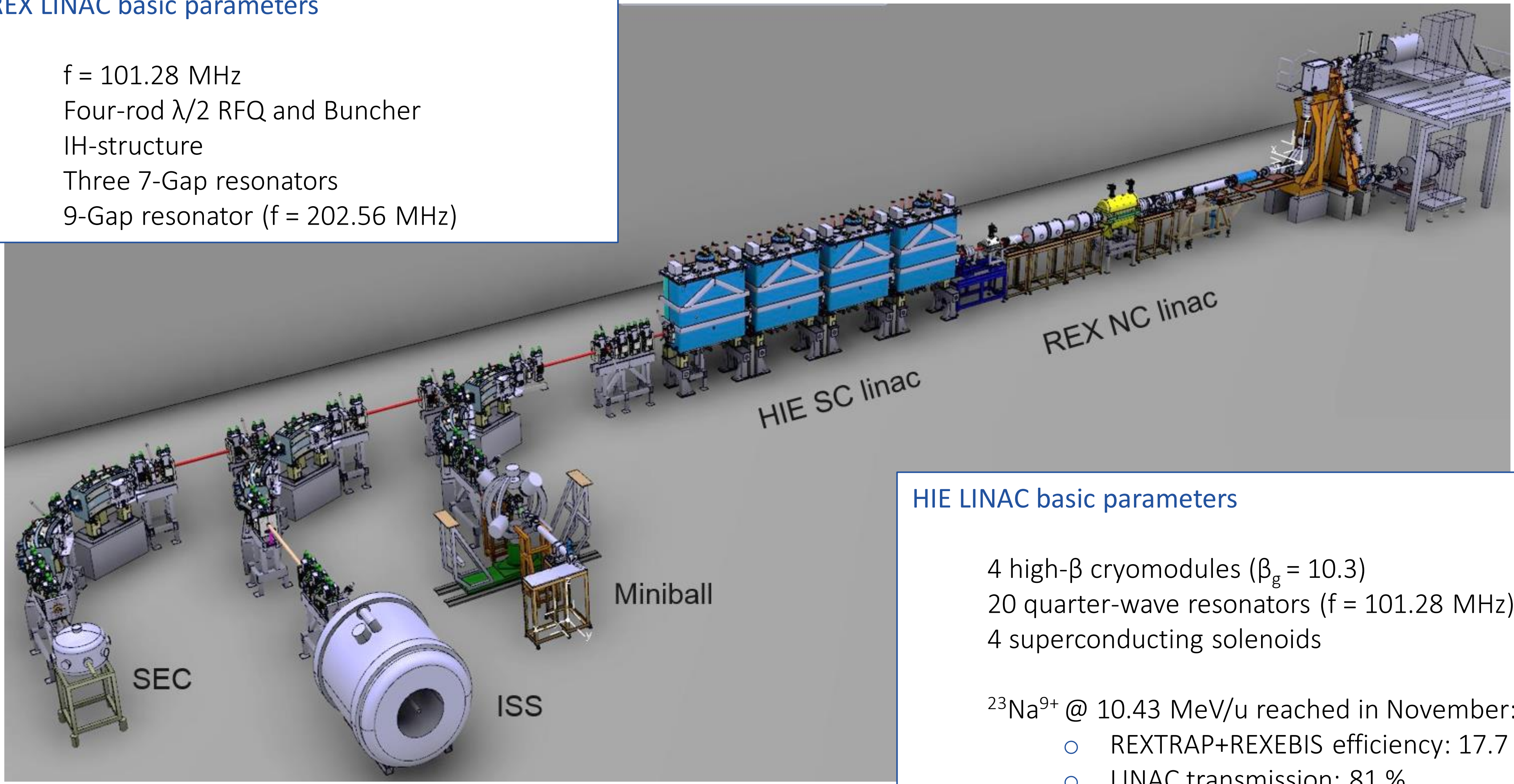

HIE LINAC basic parameters

4 high-β cryomodules (β_g = 10.3)
20 quarter-wave resonators (f = 101.28 MHz)
4 superconducting solenoids

$^{23}Na^{9+}$ @ 10.43 MeV/u reached in November:

- REXTRAP+REXEBIS efficiency: 17.7 %
- LINAC transmission: 81 %

Abundant contamination

Technique Variation of REX *A/q*-Separator magnet, monitoring of current passing through slit on Faraday cup.

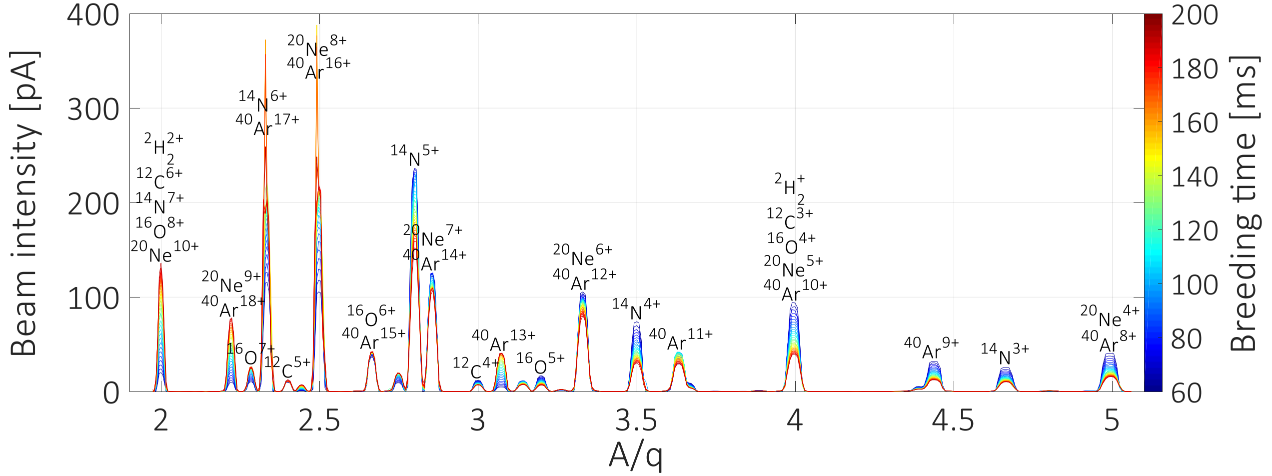

Figure Spectra obtained with previous immersed electron gun design, LaB6 cathode at I_{e-} = 200 mA and U_{gun} = 4 kV (2017).

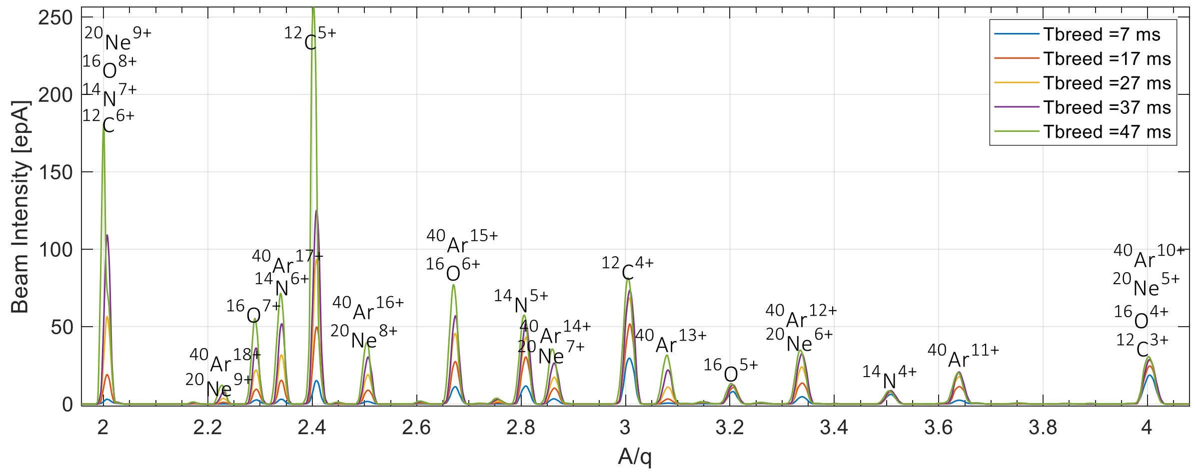

Figure Spectra obtained using non-adiabatic immersed electron gun, IrCe cathode at I_{e-} = 200 mA and Ugun = 6 kV (2020).

- Expected contamination from air. (Not labelled: ^{13}C, ^{15}N, ^{17}O, ^{18}O, ^{21}Ne, ^{22}Ne, ^{36}Ar, ^{38}Ar)
- Insights at the initial partial pressures of the components.

Charge dynamics

$$\frac{dN_q}{dt} = \frac{j_e}{e}\Big(\underbrace{N_{q-1}\sigma_{q-1}^{EI} - N_q\sigma_q^{EI}}_{\text{Electron impact ionisation}} + \underbrace{N_{q+1}\sigma_{q+1}^{RR} - N_q\sigma_q^{RR}}_{\text{Radiative recombination}} + \underbrace{N_{q+1}\sigma_{q+1}^{DR} - N_q\sigma_q^{DR}}_{\text{Dielectronic recombination}}\Big) + \underbrace{\mathbf{n_0\bar{v}_{q+1}N_{q+1}\sigma_{q+1}^{CX} - n_0\bar{v}_qN_q\sigma_q^{CX}}}_{\text{Charge exchange}} + \underbrace{N_q R_i^{esc}}_{\text{Escape rate}}$$

EBISIM - EBIS/T charge dynamics and plasma simulations

EBISIM package, collection of tools for simulating the evolution of the charge state distribution inside an Electron Beam Ion Source / Trap (EBIS/T) using Python – Hannes PAHL

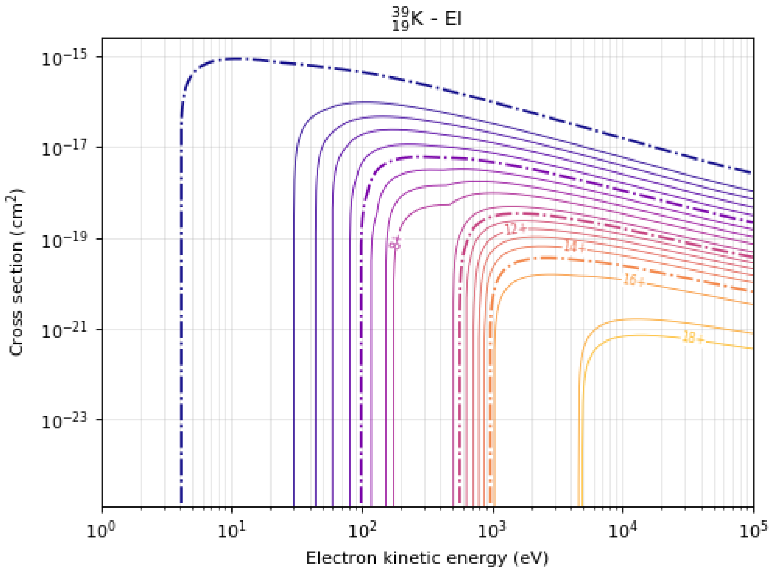

Figure Cross sections for electron impact ionisation (EI).

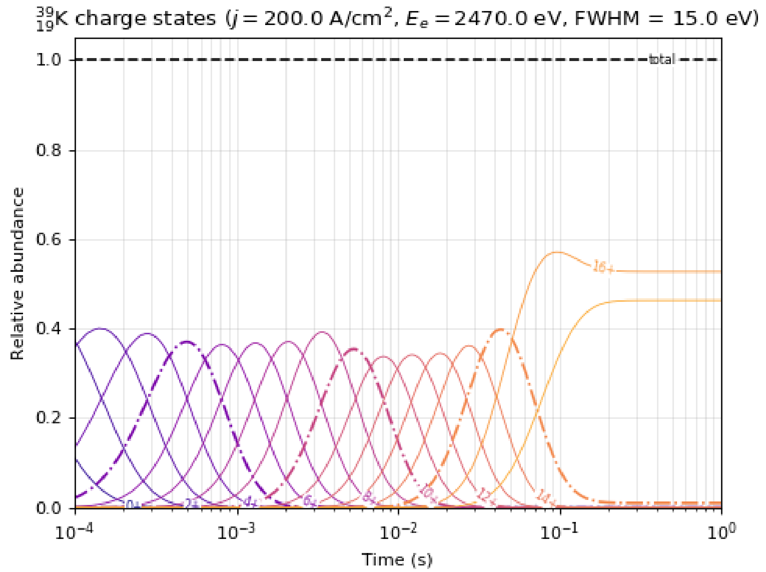

Figure Distributions of charge states of time for injected 1+ beam (EI, RR and DR).

Average potential seen $\langle \phi_i(kT) \rangle = \frac{\int q\phi\rho_i}{\int \rho_i}$

Overlap factor $f(e, i)$

Heat capacity $C_v = \frac{d\langle \phi(kT) \rangle}{dkT} = \frac{n_{DoF}}{2}$

Useful links:

Documentation (https://ebisim.readthedocs.io/en/latest/)
GitHub (https://github.com/HPLegion/ebisim#readme)

Charge state distributions

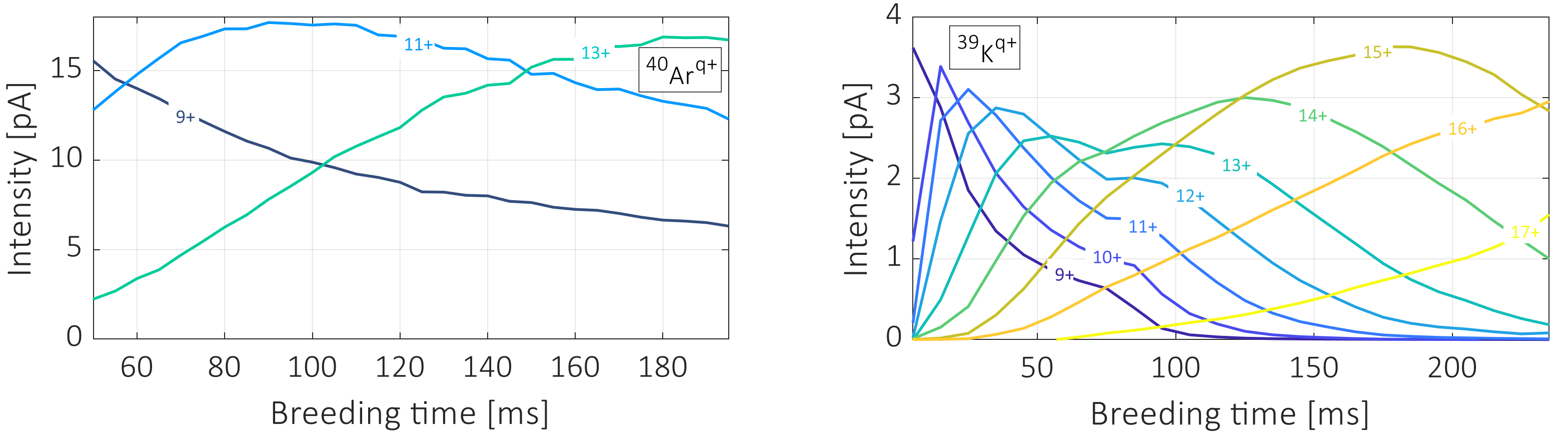

Figures Charge-state evolution as a function of breeding time for ionized residual gas (^{40}Ar) and injected beam (^{39}K).

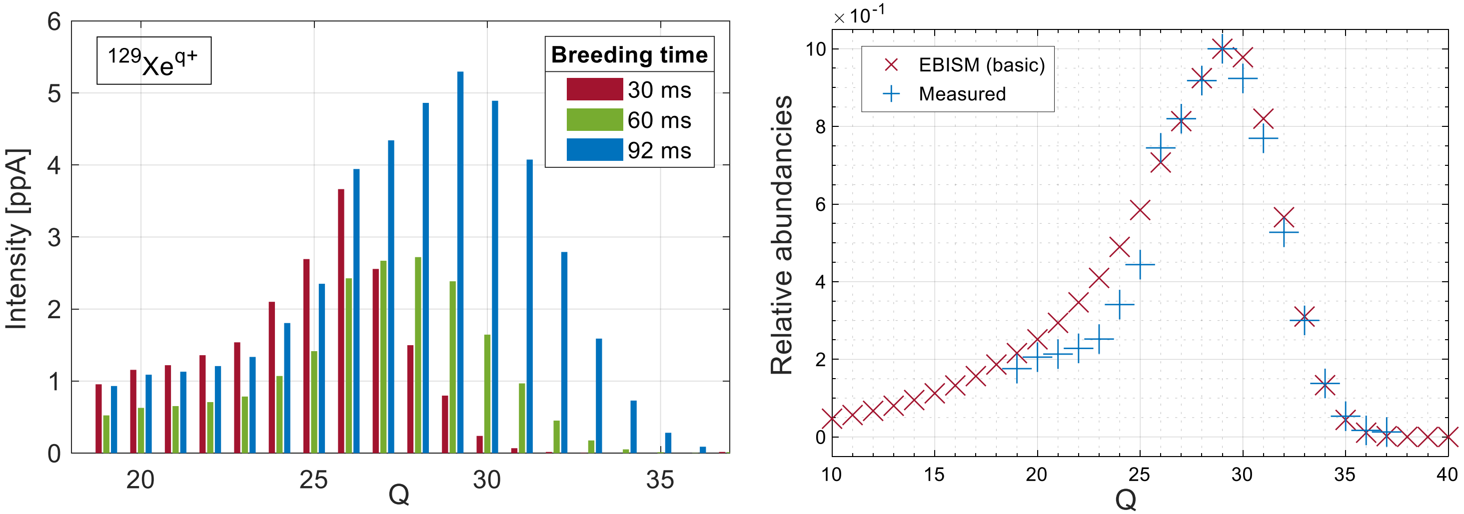

Figures CS distributions using I_{e-} = 200 mA for Xe^{q+} and comparison with simulations.

Estimate of j_{eff}, effective electron charge density, when comparing measured charge state distributions with EBISIM.

Prononced discrepancies from expected j_{eff} when the injection of the beam into REXEBIS is not optmized with care.

Fitting results between EBISIM and measurement:

- ❑ j_{eff} = 400 A/cm^2 for I_{e-} = 300 mA
- ❑ j_{eff} = 300 A/cm^2 for I_{e-} = 200 mA

From epA to single-ion detection

Technique Instead of varying REX *A/q*-Separator magnet, all necessary beam optics and RF, from REXEBIS to the Si detector, are scaled for each A/q step.

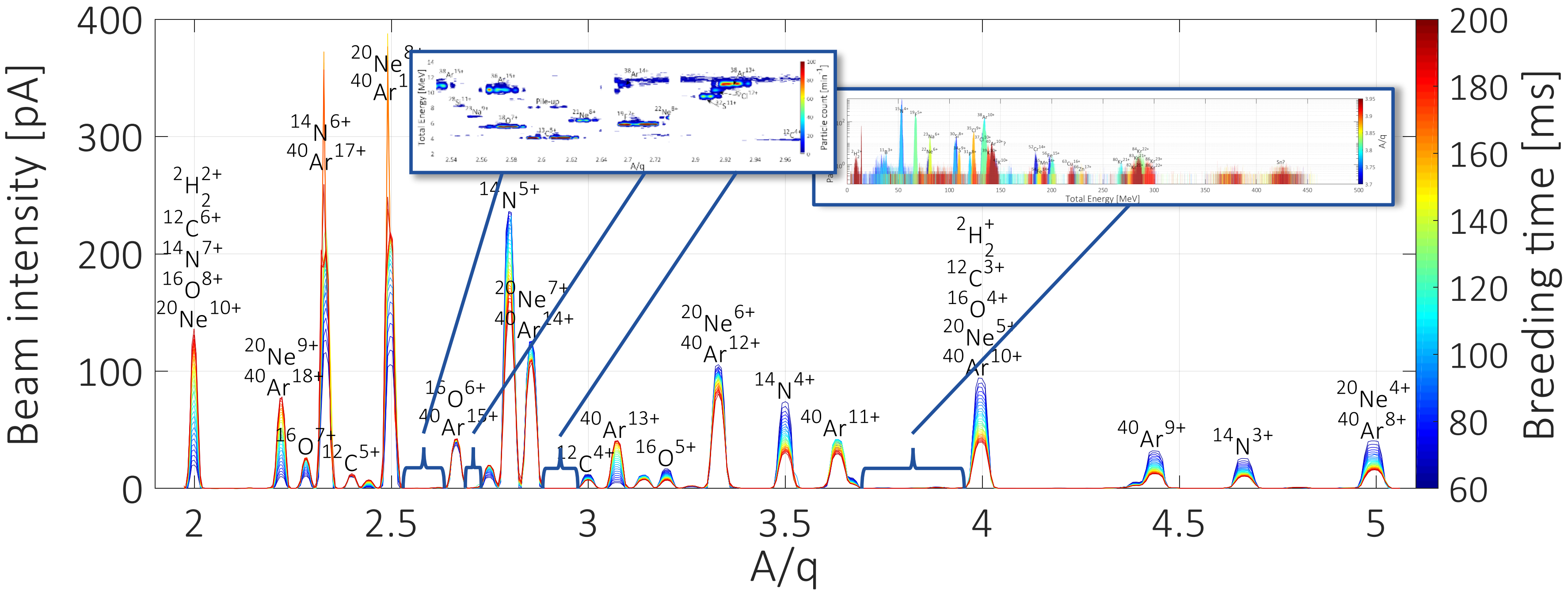

Figure Areas probed during the first tests for the conceptual proof of the method in 2017/2018.

Experimental setup in 2017/2018, using LaB6 cathode at lower electron beam density:

- Demonstration of the capability to probe rare contaminants.
- Residual gas ions were accelerated through the RFQ and transported to a Si detector.
- Intensities were not representative of reality.

From epA to single-ion detection

Results Obtained in 2017/2018 to evaluate the efficiency of probing rare contaminants across the A/q-spectra using a silicon detector.

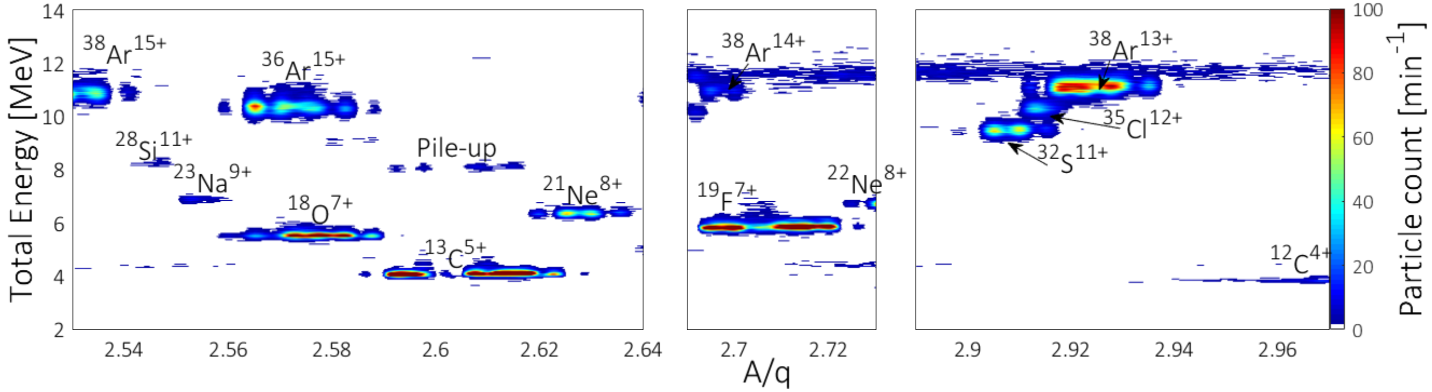

Figure Contour of energy histograms acquired on *9 mm*-SD. Beam defocused. RR = 20 Hz; breeding time = 10 ms; I_{e-} = 160 mA.

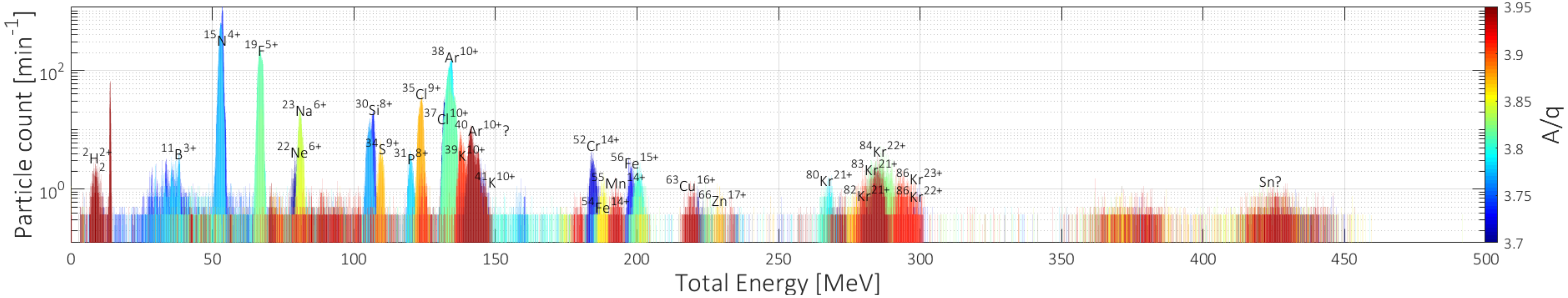

Figure Energy histograms acquired on *15 mm*-SD. Foil 5%. RR = 20 Hz; breeding time = 35 ms; I_{e-} = 140 mA.

"Residual Gas Ions Characterization from the REXEBIS", N. Bidault, *et al.,* IPAC2018, Vancouver, 10.18429.

From epA to single-ion detection

Technique Instead of varying REX *A/q*-Separator magnet, all necessary beam optics and RF, from REXEBIS to the Si detector, are scaled for each A/q step.

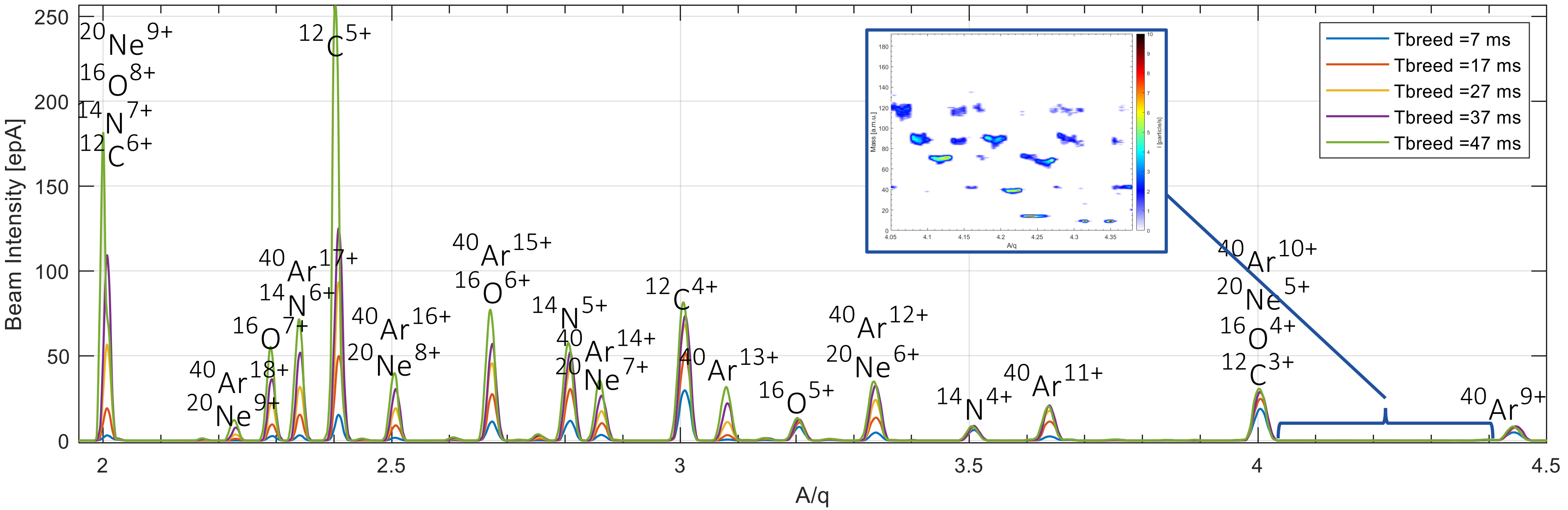

Figure Areas probed during the second batch of tests with new diagnostic boxes installes, in 2020.

Experimental setup in 2020, using non-adiabatic gun with IrCe cathode at higher electron beam density:

- Confirmation of the capability to probe rare contaminants.
- Residual gas ions were accelerated through the RFQ and acquired on a large Si detector installed directly afterward.
- Intensities are representative of reality.

Rare contaminants

Preliminary results/treatment

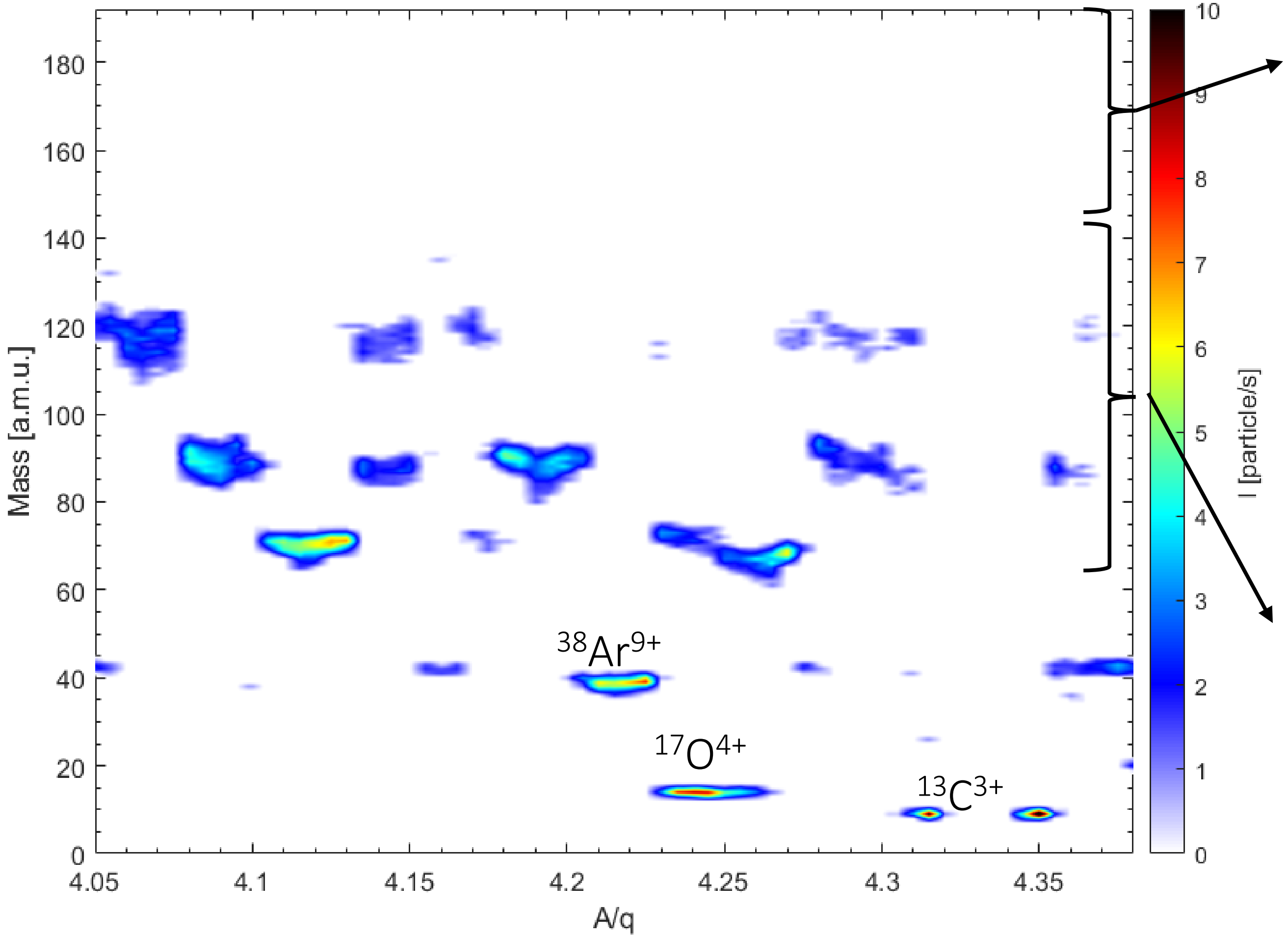

Figure Mass-scan measured with Breeding time = 45 ms; I_{e-} = 250 mA.

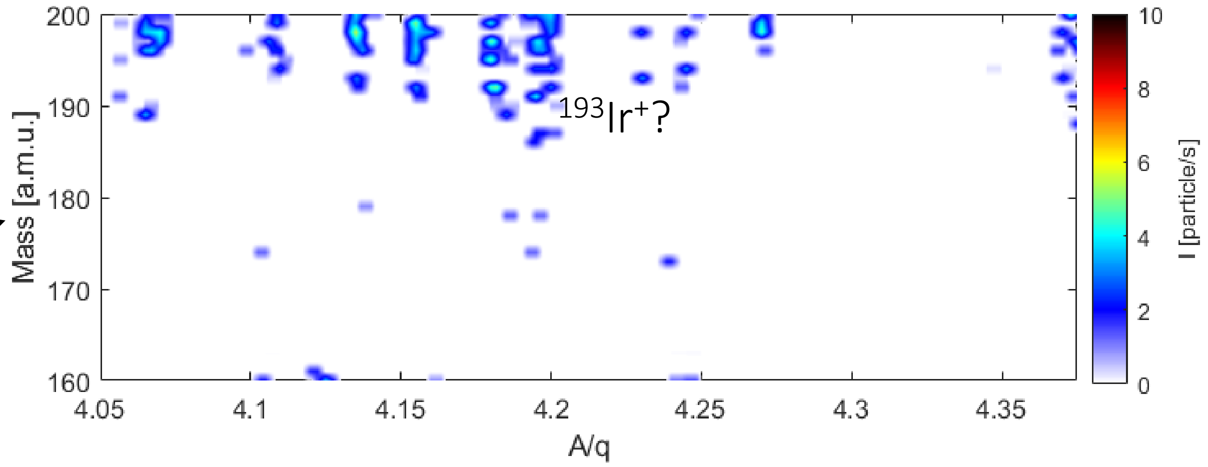

Figure Breeding time = 195 ms ; I_{e-} = 250 mA.

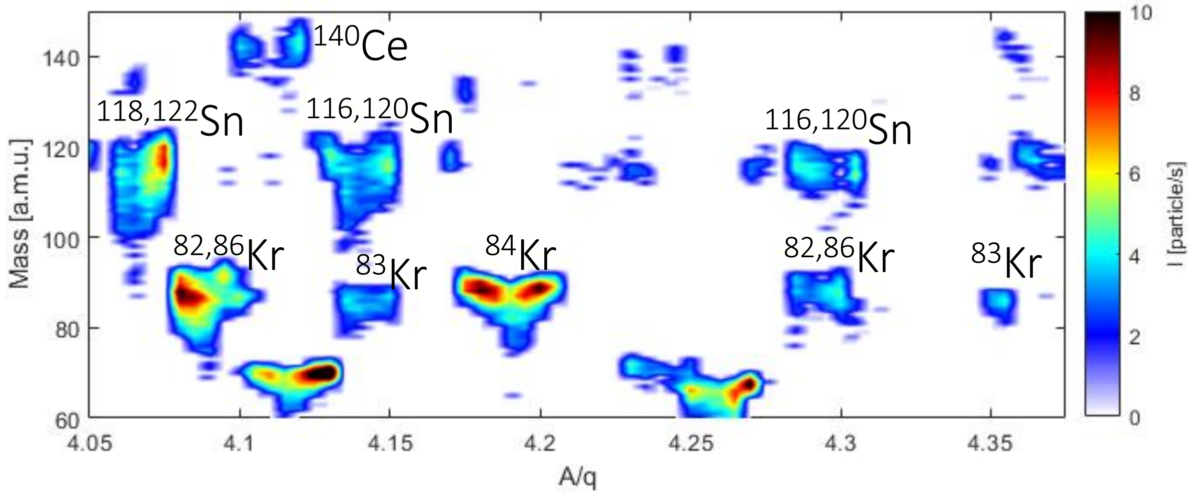

Figure Breeding time = 95 ms ; I_{e-} = 250 mA.

Axial energy distribution

Technique Variation of REXEBIS extraction potential and monitoring of escaped ions to reconstruct the axial energy distribution.

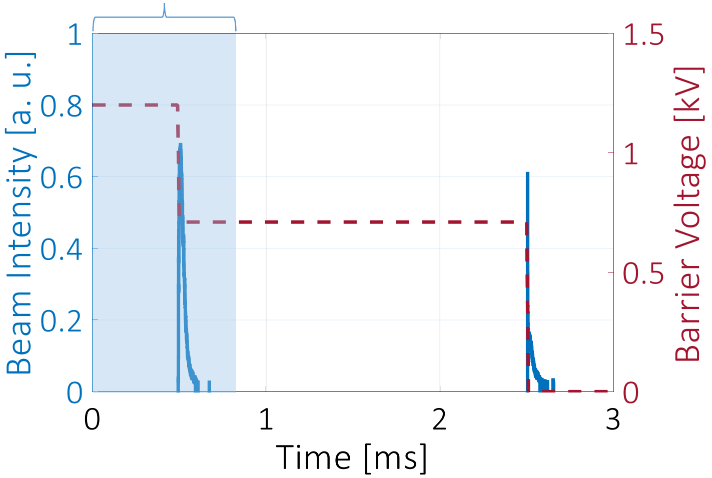

Figure Time-of-Flight measured after the *A/q*-Separator when gating with the outer barrier.

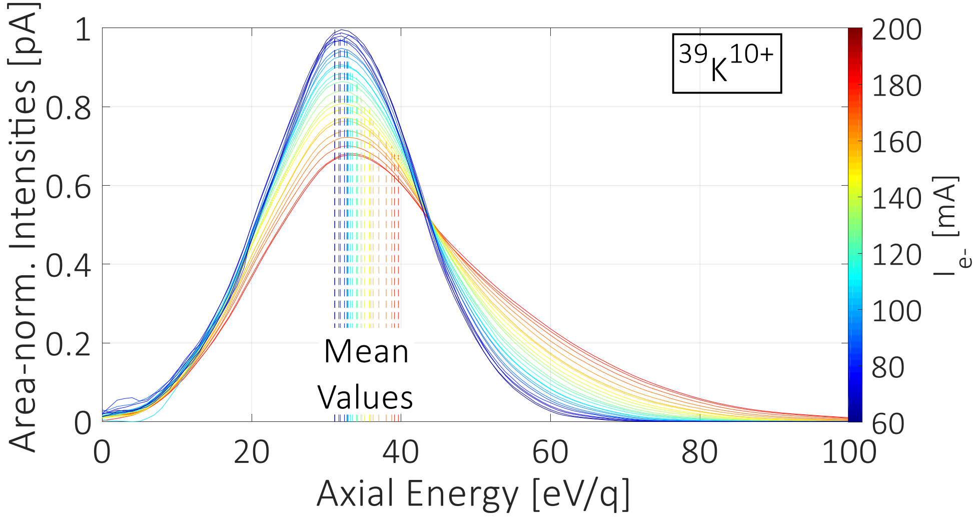

Figure Ionic axial energy distribution measured at REXEBIS extraction, as a function of the electron beam current.

Energy dynamics

$$\frac{dN_i kT_i}{dt} = \left(\frac{\mathbf{dN_i kT_i}}{\mathbf{dt}}\right)^{\mathbf{Coulomb}} + \left(\frac{dN_i kT_i}{dt}\right)^{\mathrm{Ionisation}} + \sum_j \left(\frac{dN_i kT_i}{dt}\right)^{\mathrm{Transfer}} + \left(\frac{dN_i kT_i}{dt}\right)^{\mathrm{Escape}}$$

Spitzer formalism

$$\Delta E_q^{\mathrm{axial}}(\mathrm{eV}) = \frac{e^3}{16\pi\varepsilon_0^2}\left(\frac{m_e}{M_i}\right)\frac{1}{E_e}\left[e\sum_{i=1}^{q-1}\frac{i^2}{\sigma_i^{EI}} + j_e q^2 \Delta t\right] \quad \text{and} \quad \Delta E_q^{\mathrm{radial}}(\mathrm{eV}) = 2C_\lambda \Delta E_q^{\mathrm{axial}}$$

Slow Extraction

Technique Discretization of the axial energy distribution and solve all $V_{barrier}(t_i)$ (barrier step-function) to obtain a constant escape rate.

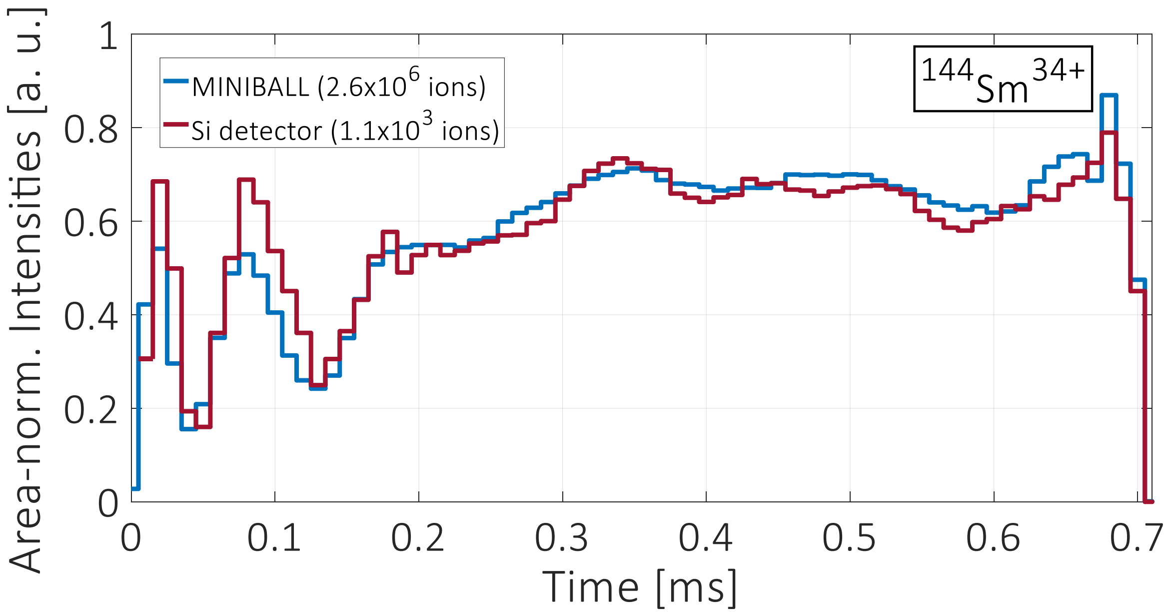

Figure Direct application of inversion formula, comparison between detectors.

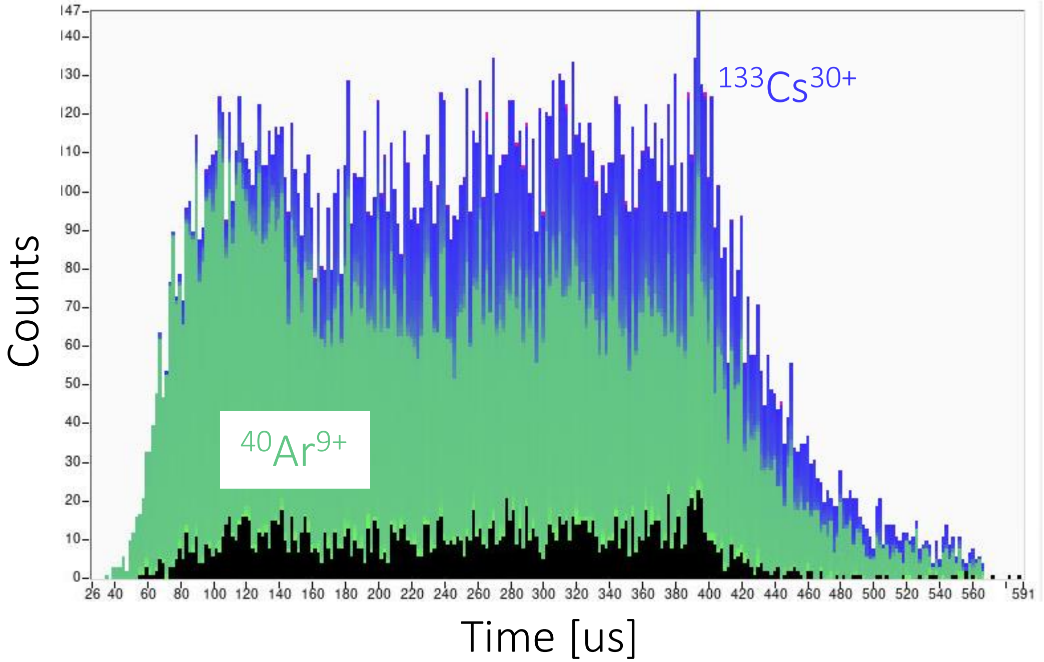

Figure Direct application of inversion formula, on a beam with contaminant.

Ion energy distribution may be assumed a Maxwell-Boltzmann with 3 DoF: $f(E_i) = \frac{2}{kT_i}(\frac{E_i}{\pi kT_i})^{1/2}\exp(-\frac{E_i}{kT_i})$

Reduction of contamation via delayed extraction of the beam of interest (high CS) ca be improved, notably with higher current density.

"Slow Extraction of Charged Ion Pulses from the REXEBIS", N. Bidault, *et al.,* AIP Conf. Proc. 2011 (2018) 070003.

HIE-ISOLDE: Transverse beam profiles at low intensity

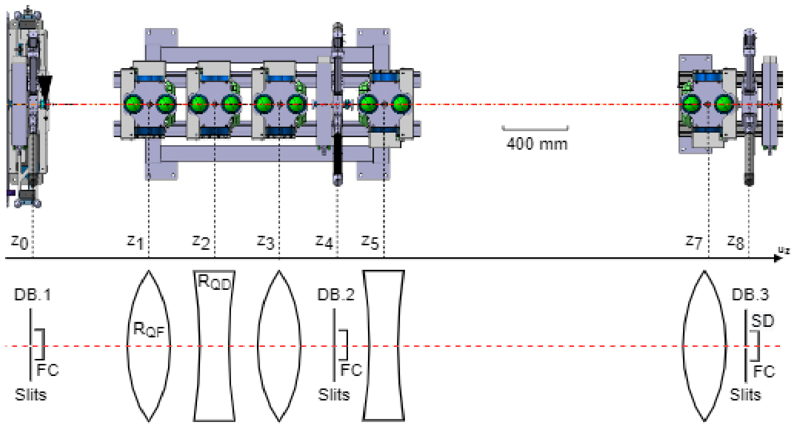

Figures Schematic of the measurement zone.

Method

- Measurement of transverse beam profiles at the same location, with a Faraday cup for pA current range or a silicon detector below 1 fA.
- Bias and exclusion (threshold) analysis.

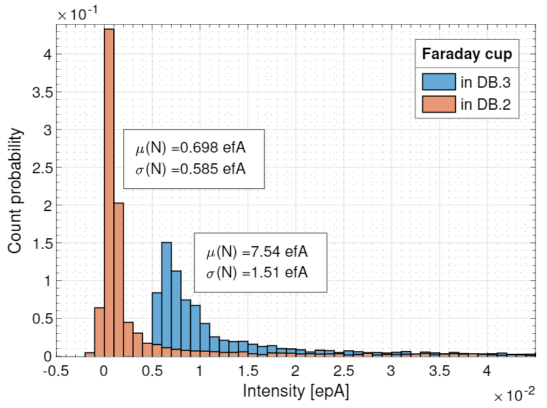

Result

Capability to measure transverse profilesof very low intensity ion beams.

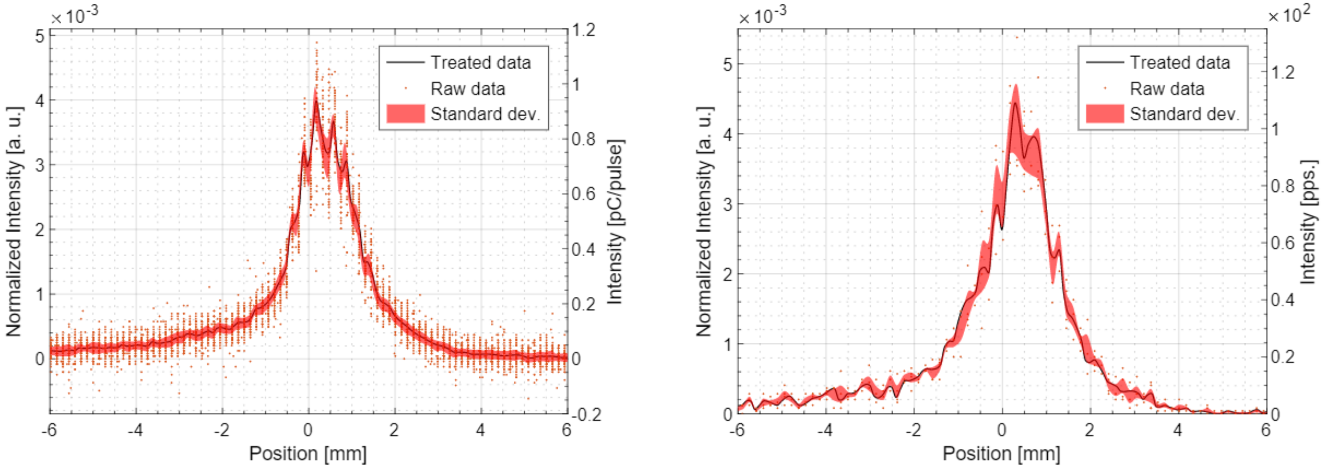

Figures Faraday cup (left) and silicon detector (right) beam profile measurements

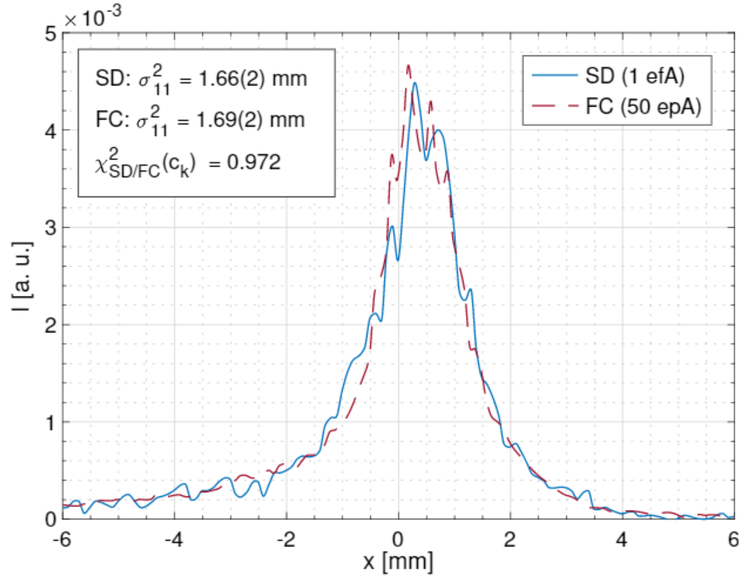

Figure Transverse beam profiles at two ranges of intensity.

HIE-ISOLDE: Transverse beam properties characterization

Experimental setup $^{39}K^{10+}$ @ 3.82 MeV/u, thin-slits and quadrupoles are used to probe the tranvserse phase-space for two ranges of intensity.

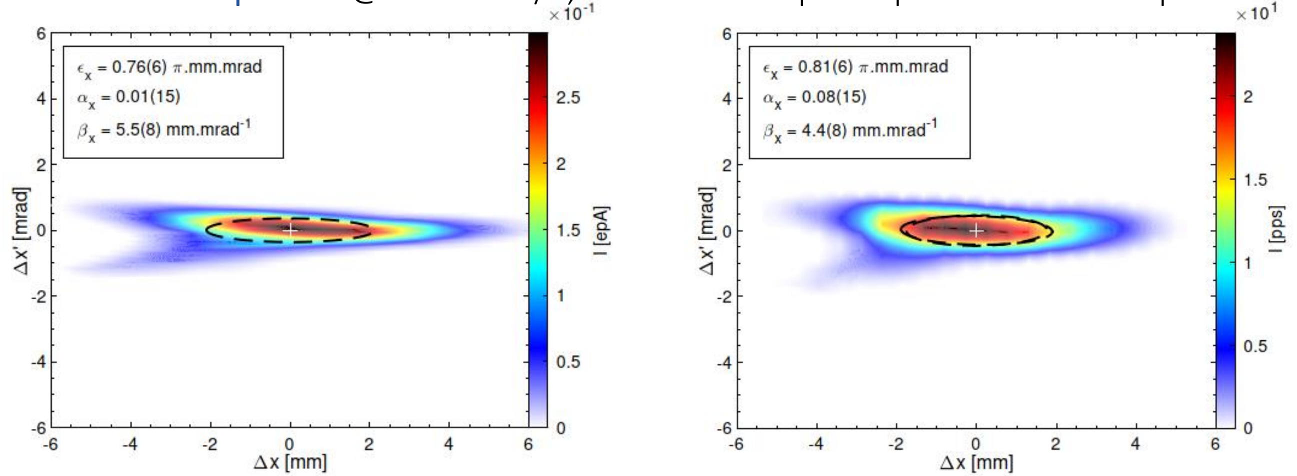

Figures Double-slit scan using Faraday cup (>10 epA) Silicon detector (<1 efA).

Method
With the double-slit scan, the transverse phase-space is sliced twice. Beamlet acquired via a silicon detector

Result
Validation of the new methodology with very low intensity ion beams.

Method
With the quadrupole scan the tranvserse phase-space is sliced once and rotated.

Result
Validation of the new methodology with very low intensity ion beams.
Tomographic reconstruction possible.

“Characterization of the transverse properties of very low intensity ion beams at the REX/HIE-ISOLDE LINAC”, N. Bidault, *et al.,* NIM-A, submitted.

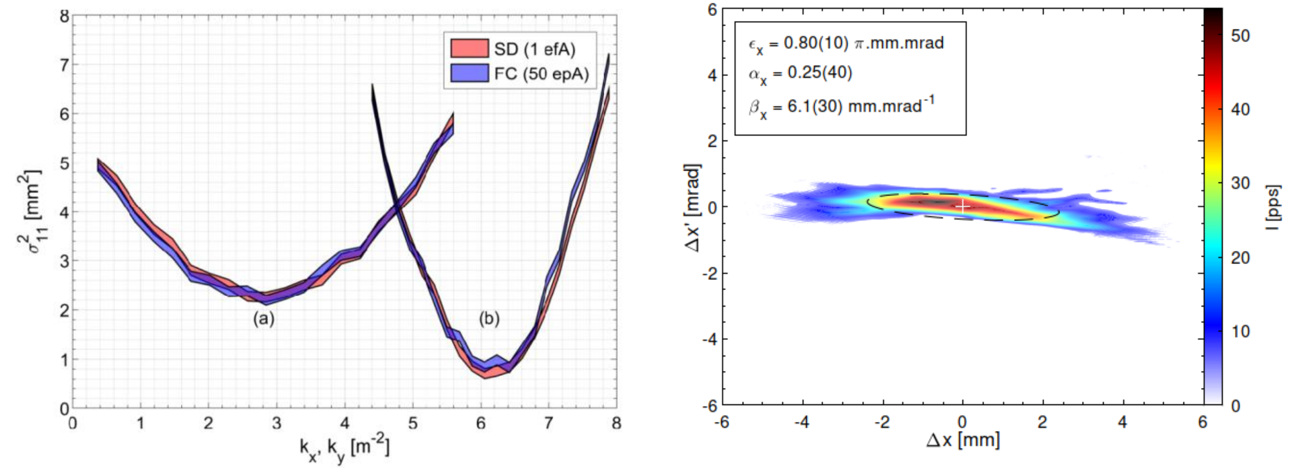

Figures Quadrupole scans for two range of intensity and tomographic reconstruction.

HIE-ISOLDE: Beam energy distribution measurement

Technique Use of an HEBT dipole as energy-spectrometer and three vertical slits. Acquisition of beamlet current by a Silicon detector.

Measurements using the three HEBT dipoles confirmed to be similar.

The energy spread derived is overestimated depending on the beam transverse emittance and the spacing between the 1-mm vertical slits.

Proven capability to measure the energy distribution of very low intensity ion beams.

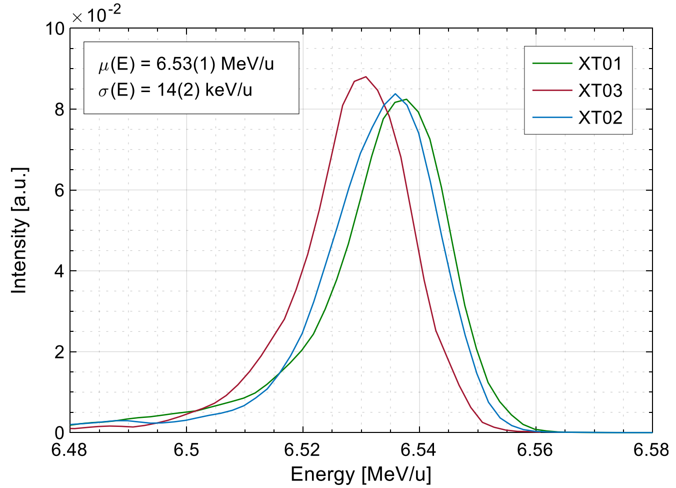

Figure Energy measured using each XT0x dipole.

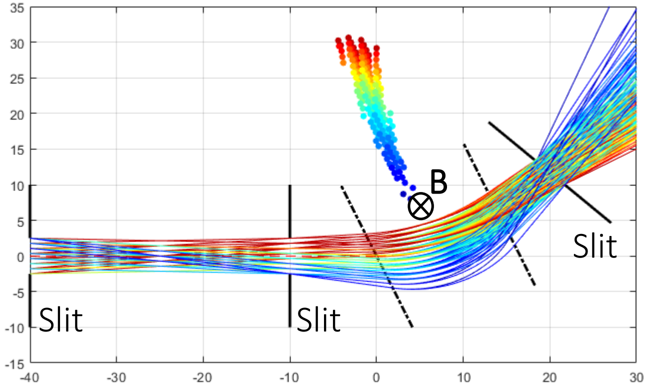

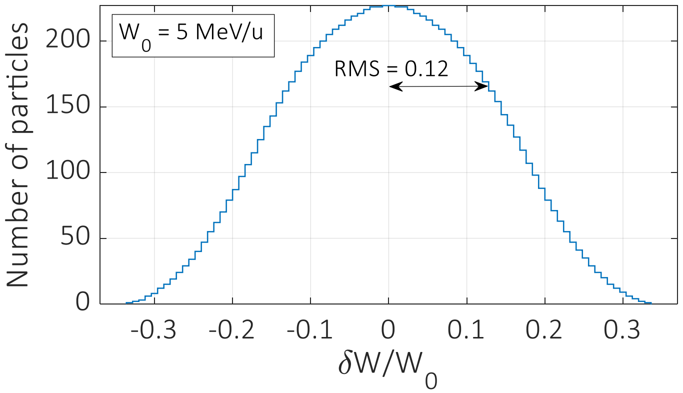

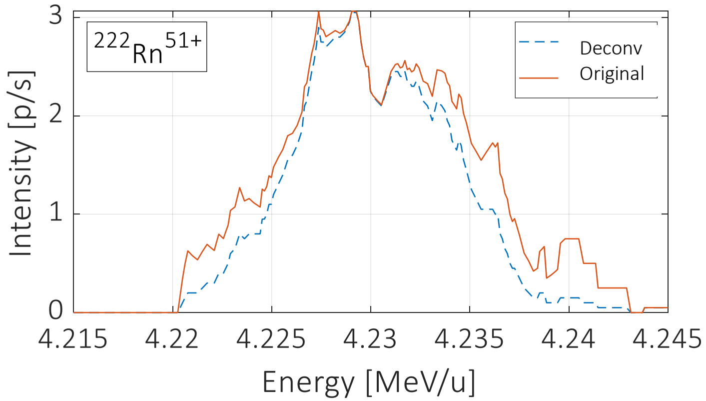

Figures Estimation the inherent spread introduced by the thin slits in the measurement channel and deconvolution on typical energy distribution measured from a RIB.

HIE-ISOLDE: Longitudinal phase-space characterization

Experimental setup $^{20}Ne^{7+}$ @ 6.64 MeV/u, 10 superconducting cavities at nominal accelerating phase, 1 SCC as Buncher at zero-crossing phase.

Method

Within beam matrix theory the elements σ_{11} and σ_{22} are quadratic as a function of the gradient of buncher cavity E_0.

Longitudinal canonical basis: $\begin{pmatrix} \Delta t \\ \Delta W/A \end{pmatrix}$

RF gap: $\begin{pmatrix} 1 & 0 \\ -q\omega_{RF}E_0TL_g\sin(\varphi_s) & 1 \end{pmatrix}$

Drift L: $\begin{pmatrix} 1 & \frac{-AL}{\beta\gamma(\gamma+1)cW_0} \\ 0 & 1 \end{pmatrix}$

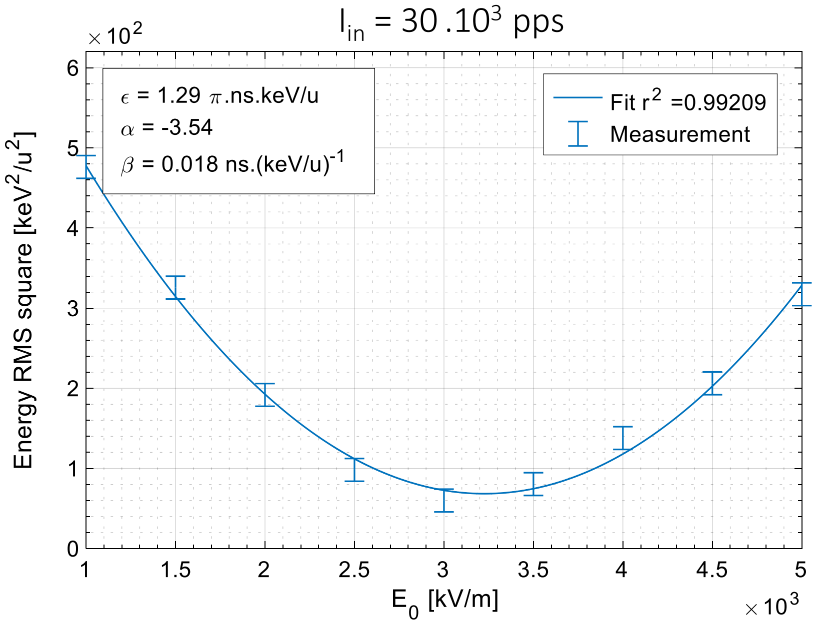

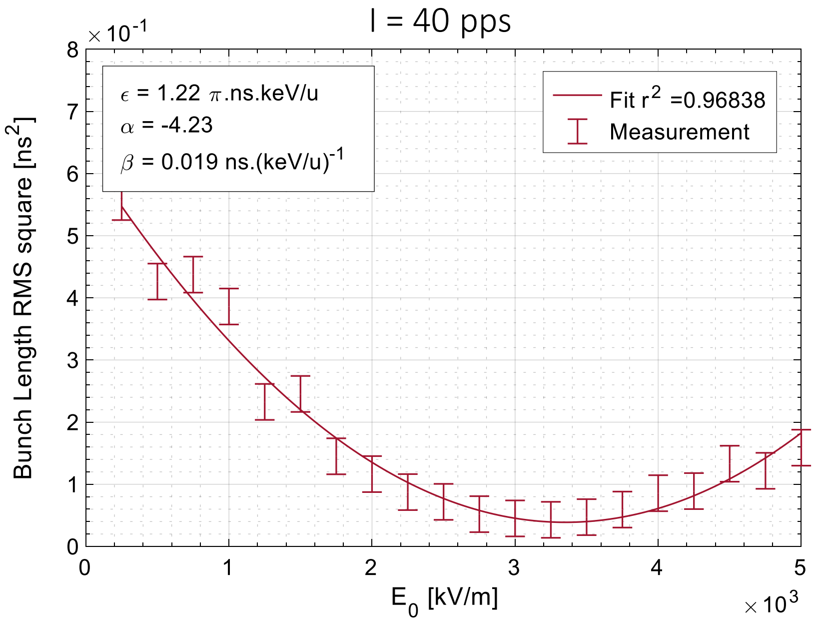

Figures Measured energy spread and bunch temporal length as a function of varying E_0.

Result

Proven capabilitity to characterize the longitudinal phase-space of sub-efA ion beams.
Correlation verified between ToF and energy-spread measurements for the longitudinal phase-space characterization.

"Longitudinal beam properties characterization of very low intensity ion beams at REX/HIE-ISOLDE", N. Bidault, *et al.,* NIM.A, in prep.

Summary

Analysis of REXEBIS performance and produced ion beam quality

Estimation of REXEBIS j_{eff} for old and new electron gun
Capability to measure rare contaminants over wide A/q range
Access to ion distribution of axial energy

Post-accelerated ion beam characterization

Reliability on transverse beam profile measurements in the sub-femto A range
Method for probing the transverse beam properties at very low intensity
Consolidation of beam energy measurement technique
Method for characterizing the longitudinal phase-space at very low intensity

Thank you for your attention

This work is the result of a collaborative effort involving different parties at **CERN**:

ISOLDE Operation (BE-ISO-OP):

Miguel Luis BENITO
Eleftherios FADAKIS
Simon MATAGUEZ
Emiliano PISELLI
Jose Alberto RODRIGUEZ
Erwin Siesling

Beam Physics (BE-ABP):

Gunn KHATRI
Hannes PAHL
Alexander PIKIN
Fredrik WENANDER

Beam Instrumenation (BE-BI):

William ANDREAZZA
Enrico BRAVIN
Sergey SADOVICH

And at the **University of Rome 'La Sapienza' (Department of Physics) and INFN:**

Mauro Migliorati
Daniele del Re

Silicon Detector specifications

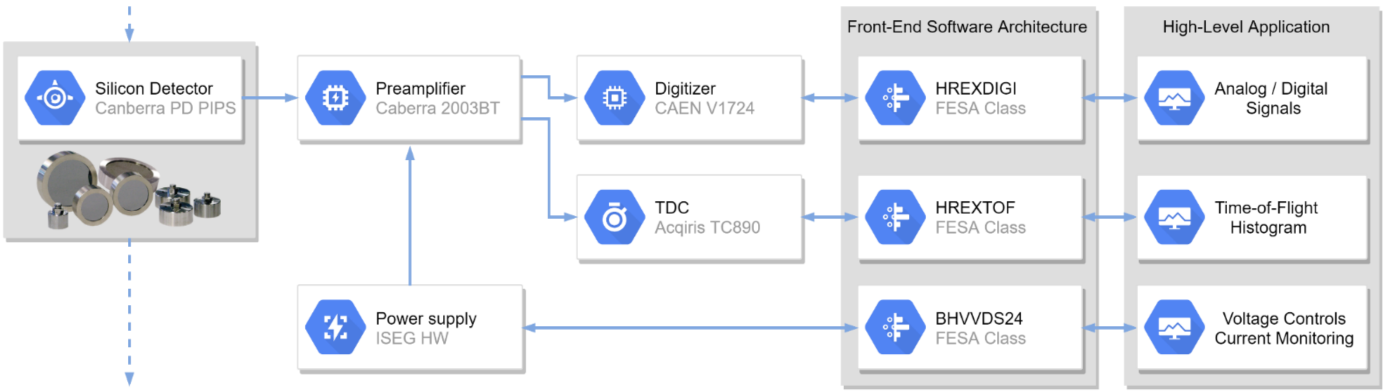

Figures Diagram of the Silicon Detectors DAQ at HIE-ISOLDE.

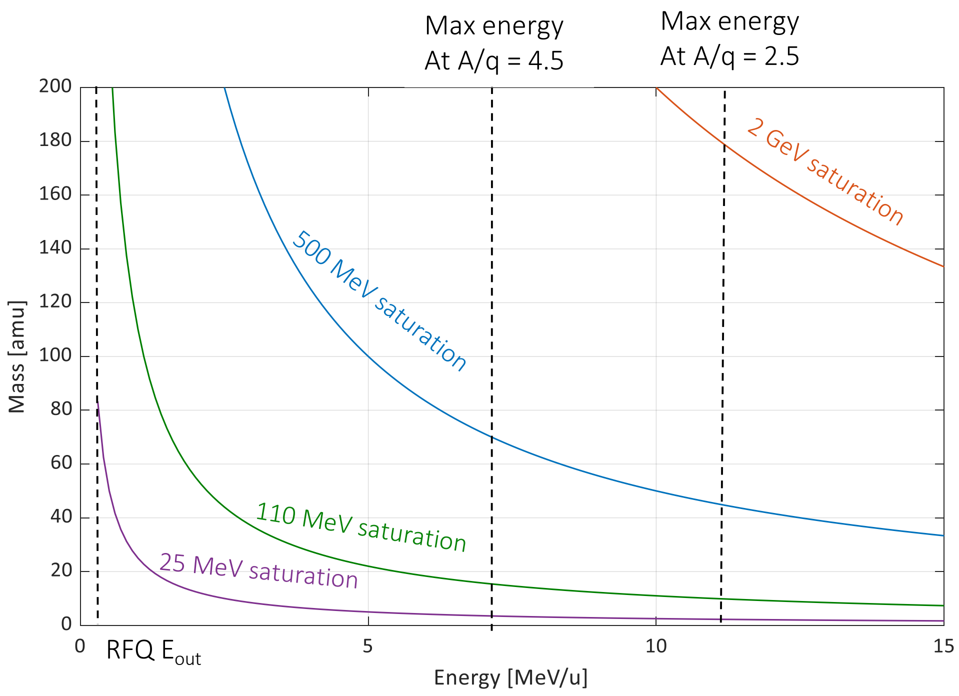

Figure Saturation curves.

Type	Canberra's model	Radius [mm]	Resolution	
			Energy* [keV]	Time [ns]
1	PD50-11-300RM	4.0	11	5
2	TMPD50-16-300RM	4.0	15	0.2
3	PD600-20-300RM	13.8	20	5

Table Basic parameters of 300 µm-thick PD-PIPS detectors used at HIE-ISOLDE (* ^{241}Am, 5.486 MeV alphas).

Silicon Detector energy resolution

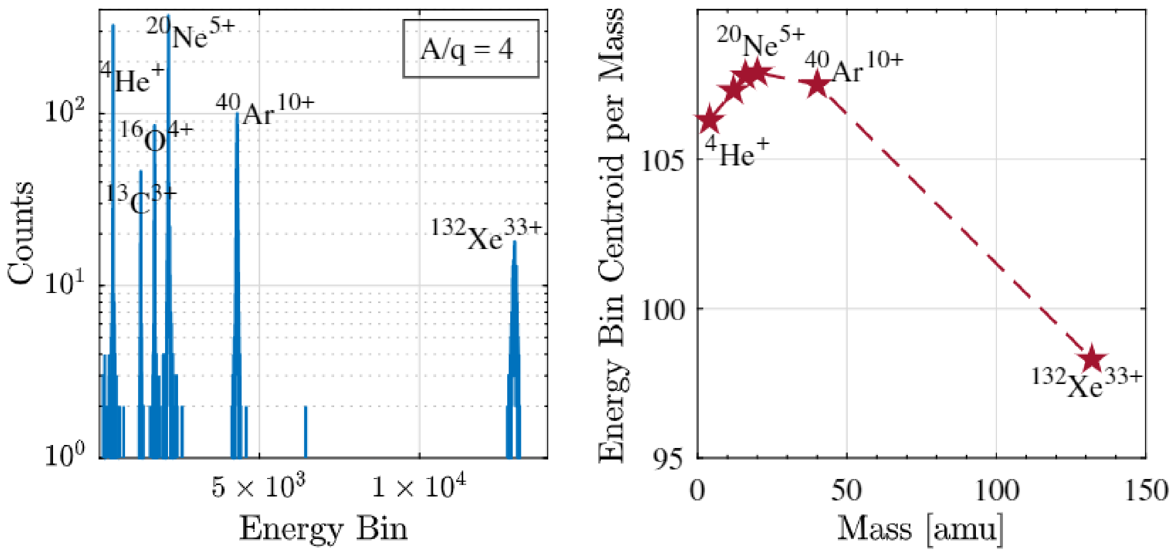

Figures Deviation of resolved energy from total energy. Measured using beam of mixed components, at W = 2.8 MeV/u

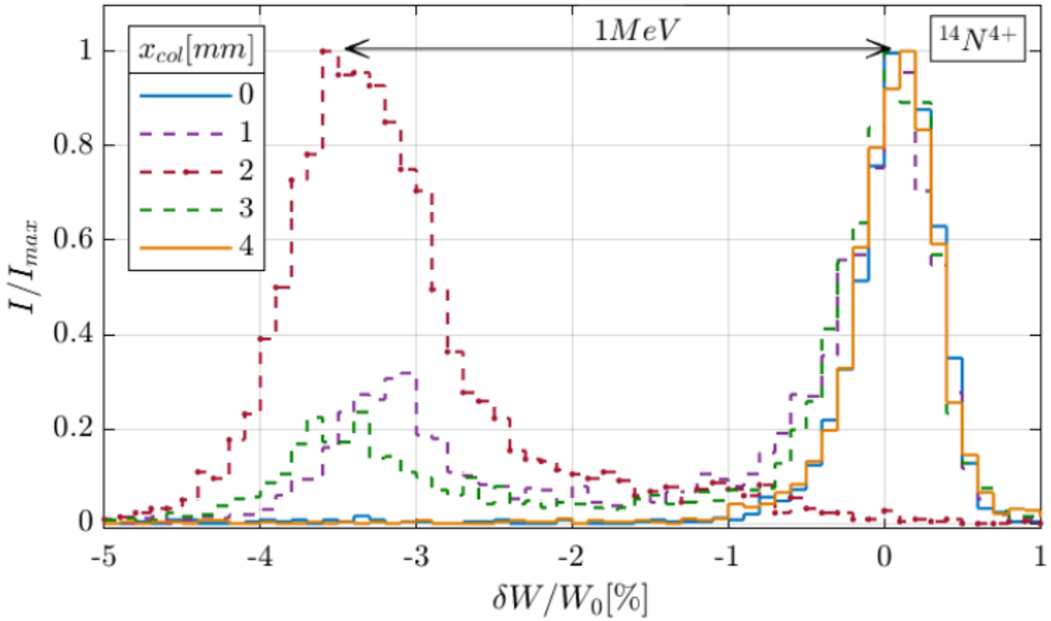

Figure Evidence of deteriotation on the silicon detector area, resulting in deviation of the measured energy.

Exclusion analysis for transverse emittance measurements

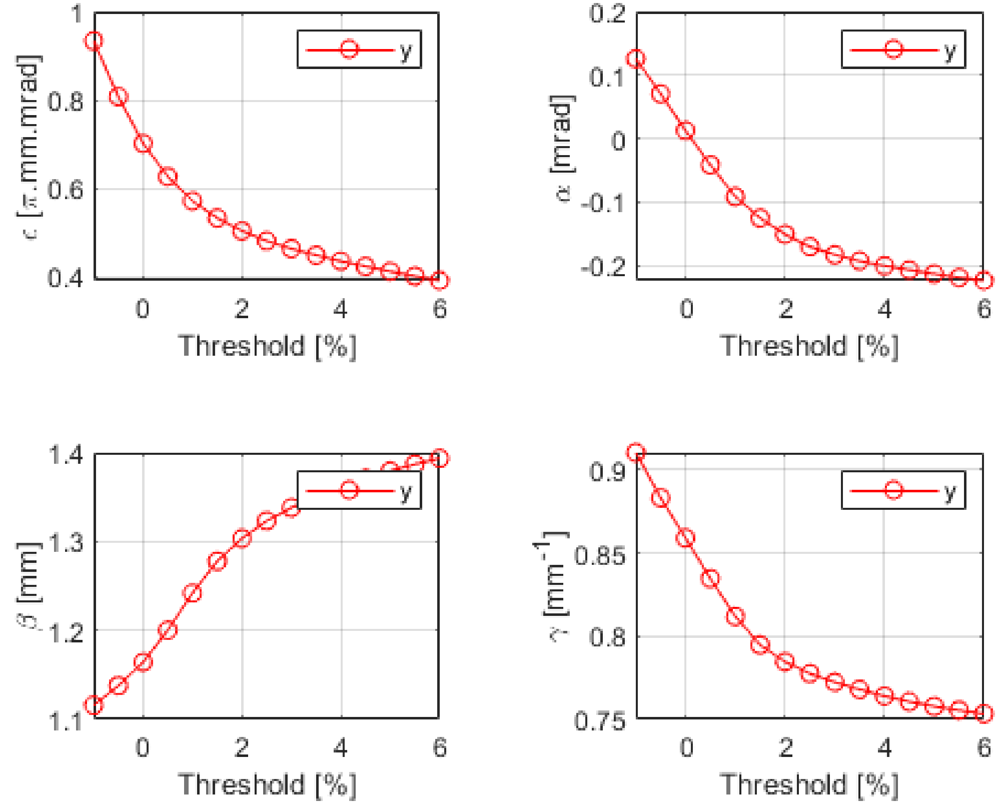

Figure Typical evolution of Twiss parameters depending on the exclusion threshold.

I_{e-} = 300 mA

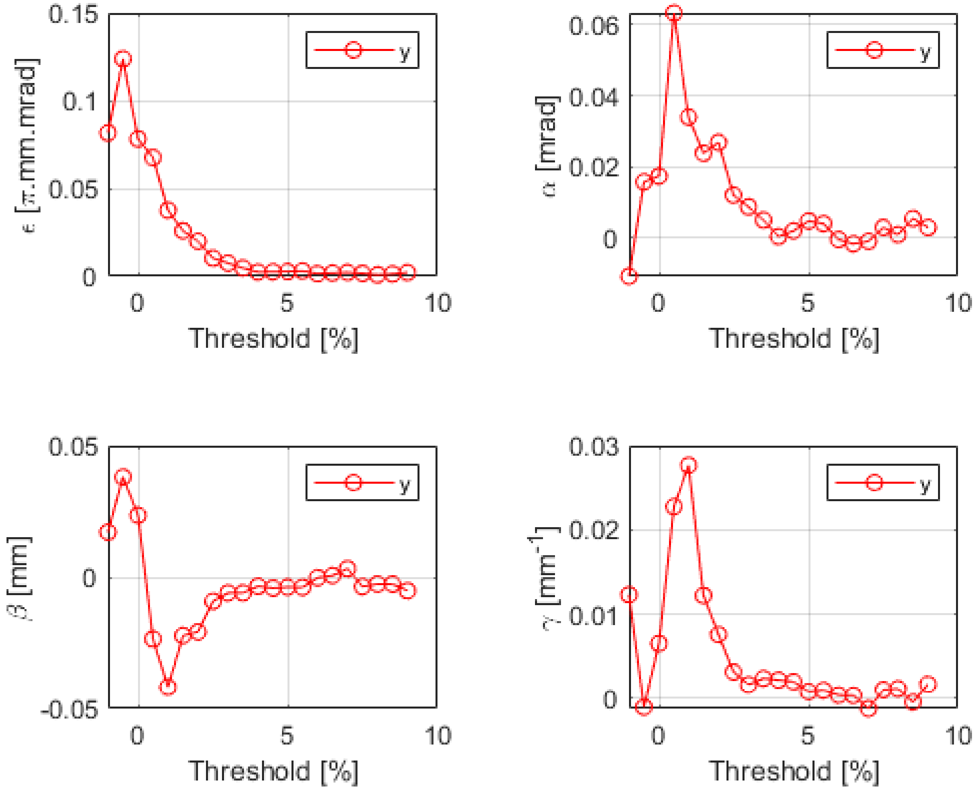

Figure Second derivative of the Twiss paramters depending on the exclusion threshold. (5% is chosen)

Non-adiabatic immersed electron gun

Design

Post anode

Iron ring

Anode

Wehnelt

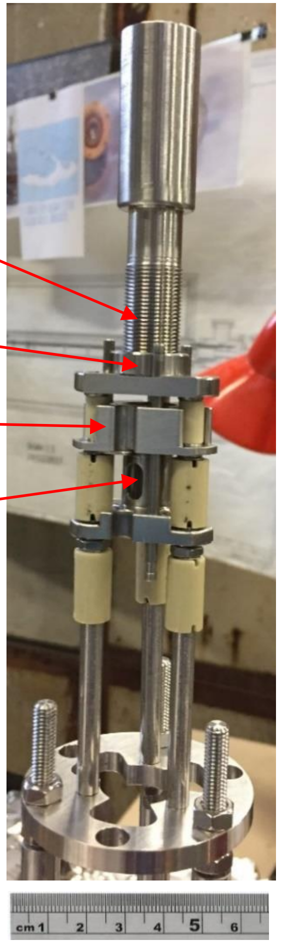

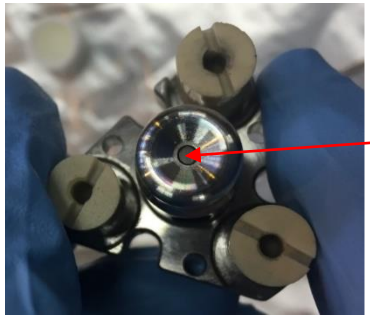

ϕ=2 mm IrCe cathode

Post anode used to adjustment the phase of cyclotron wrt iron ring for different beam currents

Results

Current and losses

I_e well behaved to 300 mA
<15 uA anode losses
<100 uA losses on drift tube in front of suppressor

EBIS breeding efficiency

19.7% for $^{39}K^{1+}$ to $^{39}K^{10+}$
Almost as high as for old gun

Effective current density

T_{breed}=44 ms for $^{133}Cs^{1+}$ to $^{133}Cs^{31+}$
j_e estimated to ~400 A/cm^2

Problems

1. Excessively high cathode work function (activation not helpful)
2. Electron beam losses rises exponentially when I_e > 300 mA. Believed to be caused by back-scattered or elastically reflected electrons from the collector region.

Non-adiabatic immersed electron gun

- Immersed electron gun positioned in low B-field (few hundred Gauss)
- Reduce cyclotron motion with local magnetic element
- Produce a laminar beam that is thereafter adiabatically compressed by main B-field

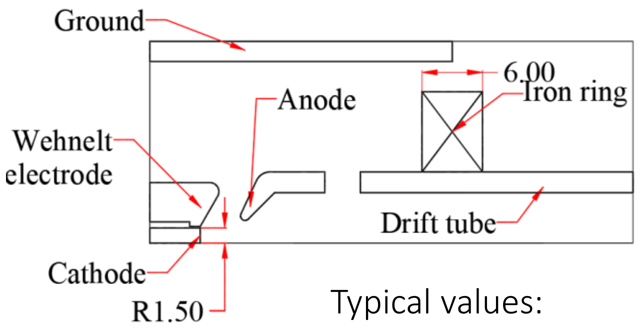

Typical values:

r_c=1.5 mm, I_e=700 mA,
E_e = 10 keV, B_{cat} = 700 Gs

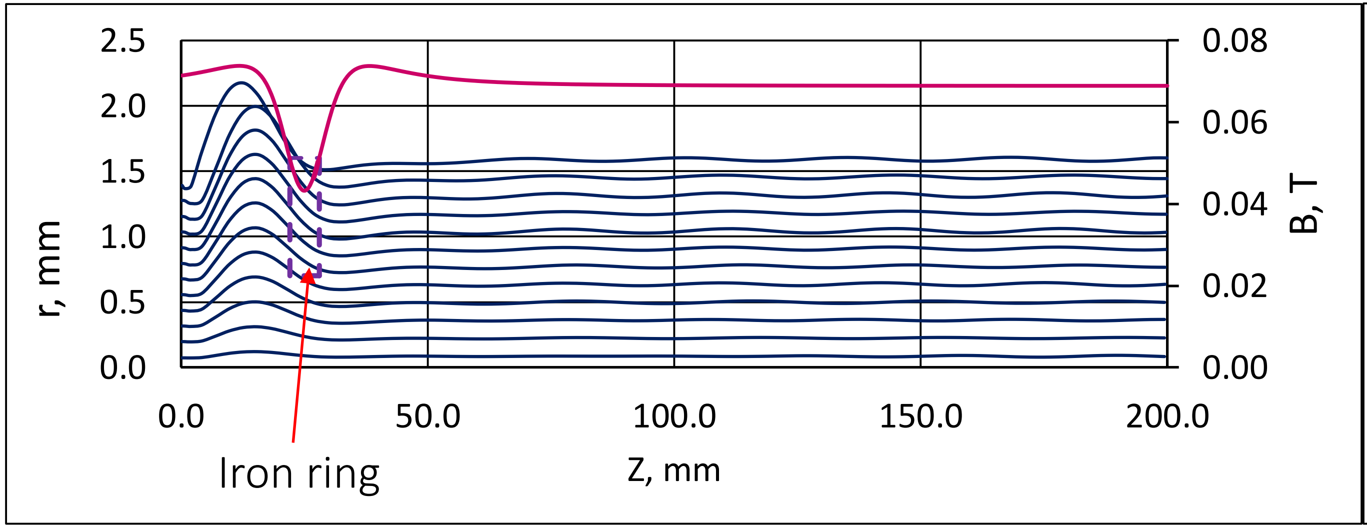

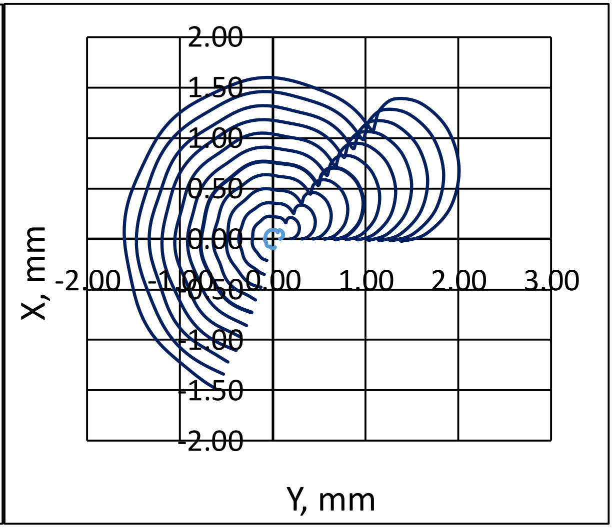

A. Pikin et al., "A method of controlling the cyclotron motion of electron beams with a non-adiabatic magnetic field", accepted PRAB

Rare contaminants

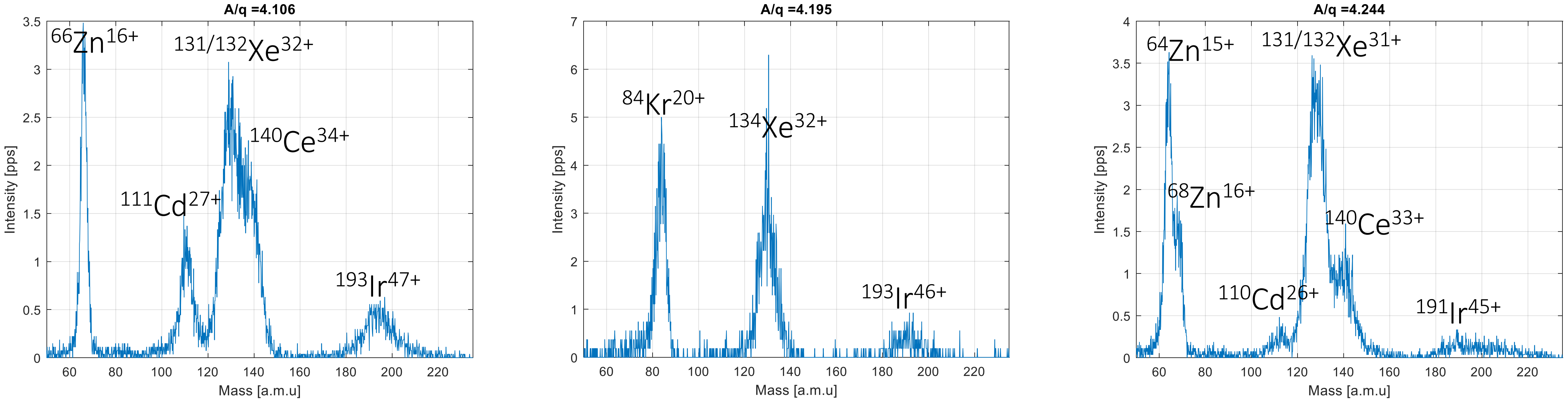

Figures Energy histogram acquired on silicon detector, with Breeding time = 192 ms and I_{e-} = 300 mA. Identification of Iridium and Cerium contamination